Eurasian Journal of Physics and Functional Materials

Volume 7 | Number 1

Article 3

Pages: 52 - 59

3-22-2023

Synthesis of silver nanoparticles by green method using ligustrum sinense to study their structural and photoluminescence properties

Sh.A. Khan
Dr. Harisingh Gour University Sagar ,India

S. Patel
Dr. Harisingh Gour University Sagar ,India

P. Shukla
Dr. Harisingh Gour University Sagar ,India

R. Kumar
Dr. Harisingh Gour University Sagar ,India

R. Dixit
Dr. Harisingh Gour University Sagar ,India ,

Recommended Citation

Khan, Sh.A.; Patel, S.; Shukla, P.; Kumar, R.; and Dixit, R. (2023) "Synthesis of silver nanoparticles by green method using ligustrum sinense to study their structural and photoluminescence properties," *Eurasian Journal of Physics and Functional Materials*: Vol. 7: No. 1, Article 3.
DOI: https://doi.org/10.32523/ejpfm.2023070104

Eurasian Journal of Physics and Functional Materials

2023, 7(1), 52-59

Synthesis of silver nanoparticles by green method using ligustrum sinense to study their structural and photoluminescence properties

Sh.A. Khan*, S. Patel, P. Shukla,
R. Kumar, R. Dixit

Dr. Harisingh Gour University Sagar, Sagar, India

E-mail: shadabanwar11@gmail.com

DOI: **10.32523/ejpfm.2023070104**
Received: 18.03.2023 - after revision

Photoelectronic devices such as solar cells require an electrolyte with electrode that has high energy conversion efficiency. Hence, ionic electrolyte and blend polymer composite electrolyte helps in ion regeneration and improving the performance of the device. Introduction of metal nanoparticles in the polymers such as the PMMA, PVDF provides this enhancement of performance. Nanoparticles are manufactured in an eco-friendly manner and characterized by UV and XRD. In this work we present the possibility that could be explored with the incorporation of nanoparticles and also see the synthesis process of green nanoparticles. The excitons dissociation in these devices could increase with the introduction of nanoparticles. They exhibit a near field surface plasmon resonance effect which couples with the existing photoactive layer, increasing the absorption cross section. We propose that these non-toxic and bio-friendly nanoparticles are very beneficial in our quest of green energy.

Keywords: nanoparticle; photoelectronic devices; polymer; biofriendly

Introduction

Nanoparticles are very important in various aspects of technology as they have provided an enormous range of applications. In physics, we study the structural properties of these nanoparticles and the many ways these properties can prove useful for different purposes. In solar cells, these nanoparticles have endowed

interesting new functions. The addition of these nanoparticles in the active layer of the cell increases the transference number of the charge carriers and also helps in decreasing the recombination rate while enhancing the dissociation of such carriers. These nanoparticles especially make a fruitful inclusion when the active layer is made up of polymers like P3HT: PCBM, PVP, PVDF, PMMA, etc. Furthermore, there are various methods to synthesise these nanoparticles where different experimental conditions (PH, temperature, mixing order, photo-sensitivity) are vital in giving the nanoparticles their special characteristics [1–3]. Some of those physical characteristics are size, shape, colour, and physiochemical properties [4–6]. Preparation of nanoparticles with plant extract has been very useful in utilising their antibacterial, and antimicrobial properties in the field of biotechnology or their optical, metallic conductor properties in the field of physics. The green synthesis of silver nanoparticles is a very safe, economical, and bio-friendly method. Green synthesis is also quite advantageous due to its high controllability of the size and shape of nanoparticles. It involves the reduction of AgNO3 with the help of juices present in the shoot system of a plant (like leaves, fruit, seeds, etc.). The multiple advantages in properties that silver nanoparticles show, like optical, electrical, catalytic, and crystalline, are due to their higher surface to volume ratio [7–10].

Silver is a transition metal with a soft texture, that is white in appearance. It is the best conductor of heat and electricity of all the known metals. It also has the best reflectivity of any metal. These properties are very useful for employing in photo-electronic devices. A good photoelectronic device requires high charge carrier mobility and excitons diffusion. These properties, along with high light absorption and carrier compilation, could be realised by using Silver plasmonic nanoparticles [11–13]. "Plasmonic", the term we use to address the charge density oscillations of the nanoparticles resulting in strong light scattering. The frequency and intensity of the surface plasmon depend upon the size, shape, size distribution, and kind of material. Surrounding temperature and humidity are also responsible for the extent of frequency observed for these surface plasmons [14]. All such properties make nanoparticles very tunable and controllable. With their enhanced physical properties, these nanoparticles become very desirable. These characteristic vibrations of the plasmon can be advantageous in increasing the efficiency of the device. The photoluminescence studies conducted for these nanoparticles exhibit peaks at 481nm and 580nm. This peak at 481nm is the characteristic peak of silver nanoparticles, indicating the absorption lines for silver [15]. The embedment of nanoparticles is done in the active layer of the device, which increases the efficiency of light scattering in the active layer. The green synthesis, as mentioned above, is the safest way to manufacture nanoparticles. In this process, metal salt is reduced from +oxidation state to zero oxidation state by the natural reducing agents like proteins, terpenoids, flavanoids, sugar, enzymes, etc. that are found in bio-extract [16, 17].

In this work, Silver nanoparticles are prepared with Ligustrum sinense leaf extract by adding freshly prepared $AgNO_3$ solution prepared in deionized water into the aforementioned extract. The extract acts as a capping agent for the nanoparticles in this process, giving the nanoparticles the characteristic properties

of Ligustrum sinense. Ligustrum sinense, also known as Chinese privet, is an evergreen plant that is toxic to animals and has low maintenance [18]. The cultivated nanoparticles are desired to provide good electro-optical properties that could be useful in preparing electrolytes.

Materials and Methods

A batch of Silver nanoparticles is fabricated by green method where Silver nitrate is reduced with the help of a leaf extract of Ligustrum sinense (Figure 1). First leaves are washed with DI water and then heated with water for 15 minutes. Then a separately prepared solution of Silver nitrate is mixed with the extract solution. After 20-30 min the formation of nanoparticles is apparent as the colour of the mixture turns reddish brown. After the formation of nanoparticles they can be centrifuged and dried to get the solid precipitate for further characterization. Samples having combination of $AgNO_3$ 10% and Ligustrum sinense extract 90% denoted Silver nanoparticles I.

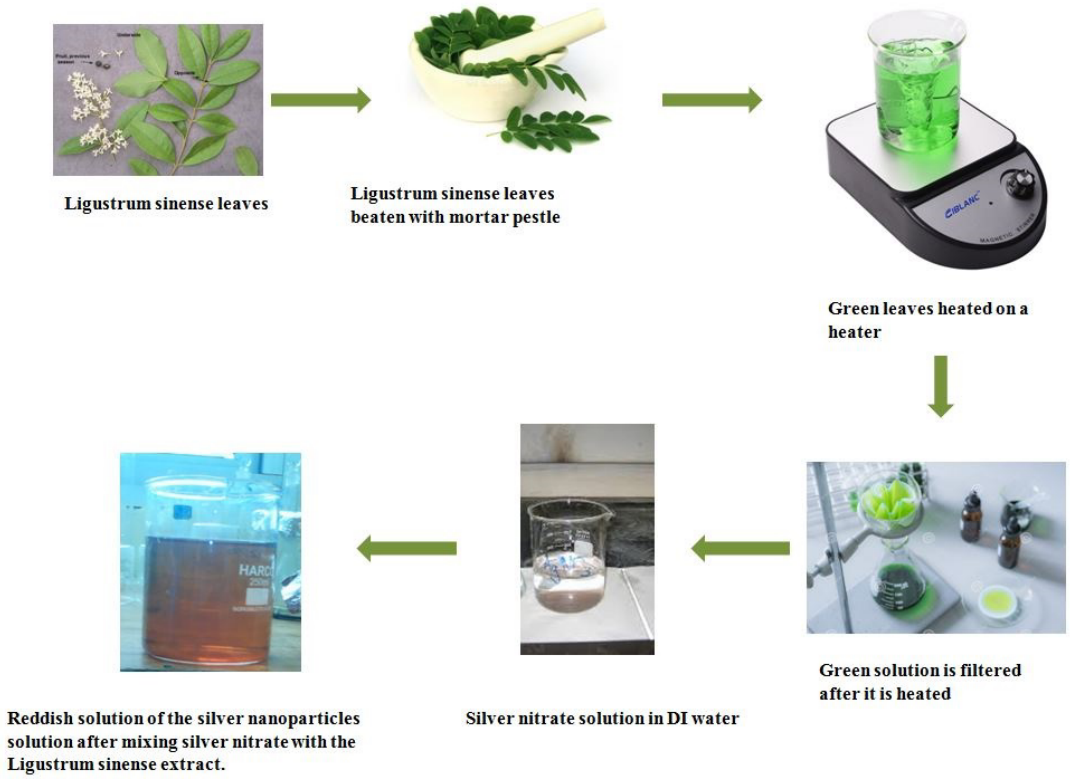

Figure 1. A schematic showing the process of preparing extract solution and mixing it with silver nitrate solution resulting in the formation of Silver nanoparticles.

Results and discussion

A liquid portion of the silver nanoparticles is tested under UV-Vis spectroscopy in the range of 200–800 nm. There is a bit of dilution involved for these nanoparticles,

and distilled water being used as the blank since distilled water is the solvent that is used in the process of the formation of nanoparticles. In the Figure 2, we can see that there is a prominent peak at 405nm as a result of surface plasmon resonance exhibited by the silver nanoparticles [19]. Springer et al. [20] also reported a similar peak for a Silver layer signifying volume plasma edge. The Kubelka–Munk function is used to calculate the optical band gap of these nanoparticles. Absorption coefficient of the sample is plotted in relation to the energy, which is known as Tauc plot. Tauc relation states the relation between the optical band gap and the absorption coefficient that is given by the

$$\alpha E = B(E - Eg)^n, \tag{1}$$

where B is a constant, E is photon energy, Eg is the energy band gap and n is a number that designate electronic transition between valance and conduction bands [21, 22]. Jan et al. [19] reported a very similar trajectory of the tauc plot where tangent to the first curve (lower energy) is extrapolated to intersect the x axis resulting in optical band gap. The variation of absorption coefficient with optical energy is shown in Figure 2(b). The estimated direct optical band gap for these green Silver nanoparticles was 2.58eV. Similar values (2.1-2.6eV) are reported by Aziz et al. [23], Hendi et al. [24] and Motitswe et al. [25] for Silver nanoparticles synthesized via green synthesis.

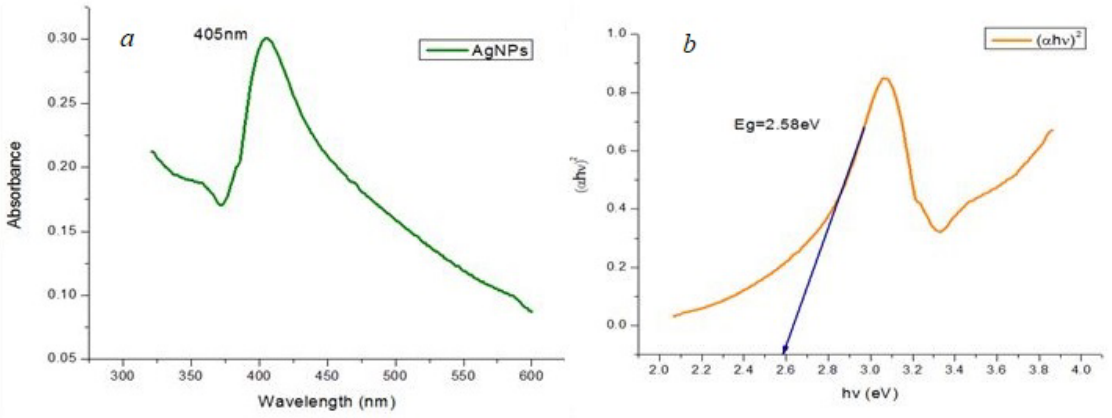

Figure 2. a) UV-vis absorbance spectrum for the nanopaticles synthesized by green method using Ligustrum sinense leaves extract b) Tauc plot for the same sample showing the direct optical band gap of 2.58 eV.

Since water is the solvent in this reaction, it can be presumed that the nanoparticles are in a "truer" position and are safer. This spectrum depicts the XRD pattern of nanoparticles produced using the green technique and leaves from Ligustrum sinense. It shows the typical peak of metallic silver at 38.5 ° (Figure 3) at (111) hkl values (JCPDS card 04-0783) with cubic structure as well as a peak at 18.38 ° that indicates the presence of flavanoids in Ligustrum sinense leaf extract, which also serves as a capping agent for the nanoparticles. Again, extremely crystalline and monodispersed nanoparticles can be seen in the sharp peak [26].

In the photoluminescence spectra, the sample with Silver nanoparticles at the excitation wavelength of 343nm shows peaks at 481 nm and 581 nm. The luminescence of Silver nanoparticles is generally attributed to the transition from the d band to the lower sp conduction band. The luminescence of silver metal is

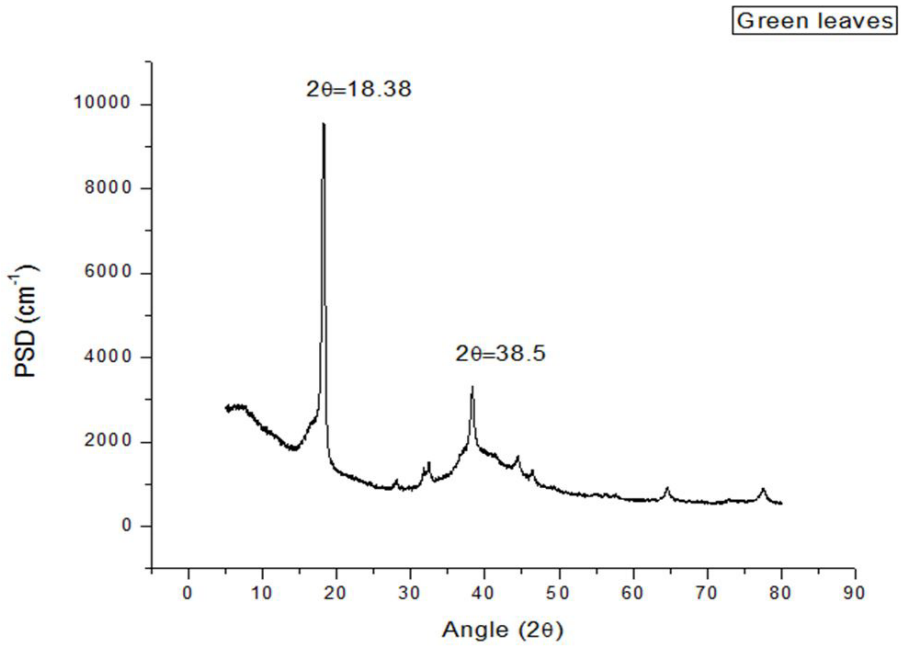

Figure 3. XRD spectrum of Silver nanoparticles prepared using Ligustrum sinense extract showing intense peaks at 18.38 ° and 38.5 °.

caused by the irradiation of an electron, a photon, or a laser. Plasmon absorption, which is characteristic of Silver nanoparticles, is observed at 481 nm. Band gap calculated using the photoluminescence data gives an optical energy band gap of 2.57 eV (Figure 4) which is in excellent agreement with the band gap calculated using UV-Vis data. This fluorescence may be attributed to the complexing effect between Silver ions and the flexible characteristics of organic components and the biopolymer chain of diterpenoids that contain retinol and sclareol [27].

Each luminescent material has a distinct CCT which is representative of temperature of white colour. It also explains the source of light and the amount of heat in the light emitted by the sample. CCT value is large for cold region and low for hot region. Any value over 4000K for the colour correlated temperature (CCT) designates cold region. Its values are calculated using McCamy Empirical formula [28],

$$CCT = 449n^3 + 3525n^2 + 6823n + 5520.33, \quad (2)$$

where $n = (x - xe)/(y - ye)$ is the reciprocal of slope line, (x, y) are the computed CIE coordinates for AgNPs (0.29, 0.29) and $xe = 0.3320$, $ye = 0.1858$. CCT for these Silver nanoparticles was calculated at 8932K (Figure 5). Duv is short for "Delta u,v" which describes the distance of a light colour point from the black body curve. A negative value of Duv indicates that the colour point is below the black body curve (in the range of magenta or pink), and a positive value indicates a point above the black body curve (in the range of green or yellow) [29]. Duv values between -0.006 and $+0.006$ are considered acceptable, whereas the range between -0.003 and $+0.003$ is preferred for more advanced applications. Here Duv value was calculated to be -0.0049. Moreover Colour purity is calculated using eq. given below.

$$\text{Colour Purity} = \sqrt{(x - x_n)^2 + (y - y_n)^2} / \sqrt{(x_I - x_n)^2 + (y_I - y_n)^2}, \quad (3)$$

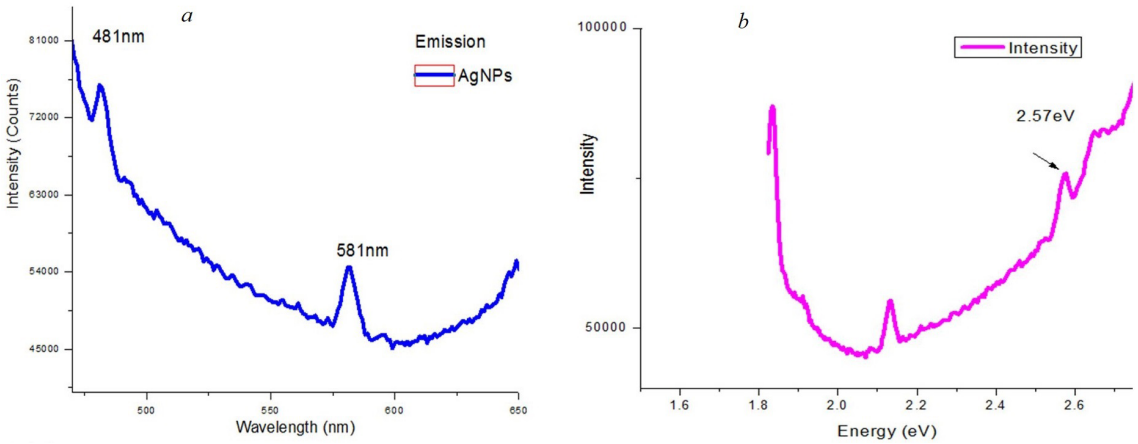

Figure 4. a) Photoluminescence emission spectra for Silver nanoparticles at the excitation of 343 nm. b) Energy spectrum obtained using photoluminescence emission spectra photoluminescence CIE diagram for AgNPs exhibiting CCT 8932 K.

where (x, y) are the coordinates of sample presented here, (x_n, y_n) are points on the chromaticity of white light (0.3333, 0.3333) and (x_I, y_I) are the points corresponding to the dominant wavelength. Colour purity of the corresponding emission spectrum for these nanoparticles was calculated at 18.8%.

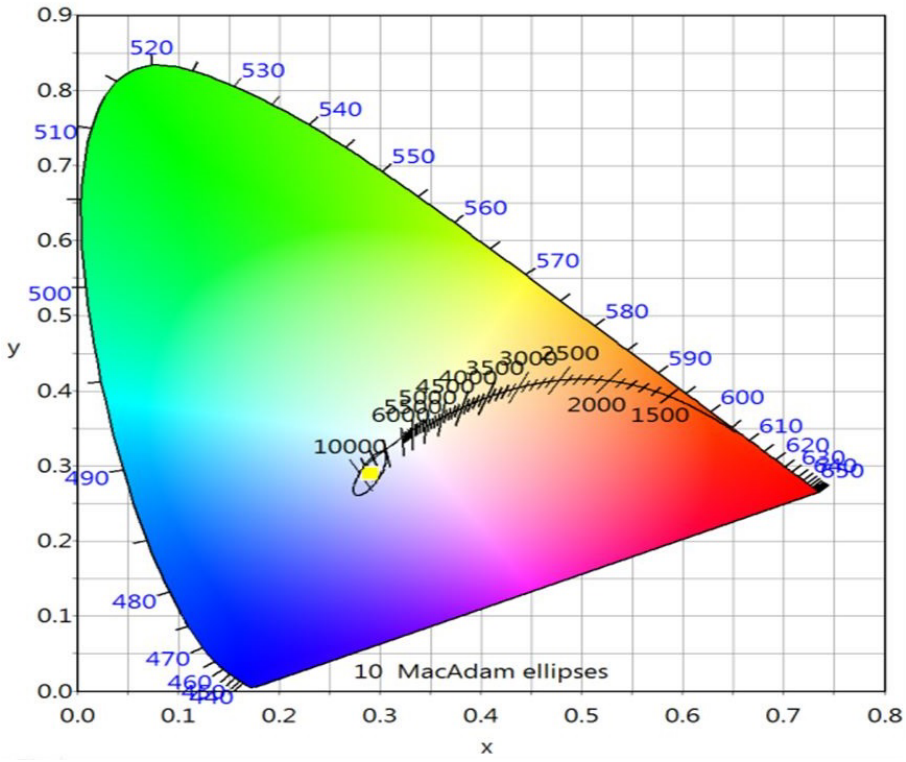

Figure 5. Photoluminescence CIE diagram for AgNPs exhibiting CCT 8932 K.

CRI (Colour Rendering Index) represents the quality of the spectrum of the light source. It plays a vital role in describing the character and composition of the spectrum of light source. CRI values of 90 or higher are generally considered excellent and below 90 are seen as poor normally. Generally CRI (Colour

Rendering Index) is calculated by

$$\mathrm{CRI} = (1/8)\sum_{i=1}^{8} R_i, \tag{4}$$

where, R_i is the special colour rendering index for each colour [30]. In this work calculated CRI general value was 96 exhibiting a great quality of light source. CRI values greater than 90 may be crucial for applications involving indoor colour appearance. Lights in this range of CRI are considered high CRI lights.

Conclusion

Silver nanoparticles were manufactured with Ligustrum sinense extract without any added toxic chemicals via green synthesis. It was observed that the peak of UV-Vis spectroscopy is sharp and narrow, showing a quite homogeneous size distribution of nanoparticles. Direct optical energy band gap (2.57 eV) was calculated using a Tauc plot, which was further reaffirmed from photoluminescence data. From the XRD study of these particles, we can infer that the nanoparticles are well formed with a crystalline structure and a cubic structure of (111) with a peak at 38.5°. CCT, CRI, and colour purity were calculated using photoluminescence, where xy coordinates for the sample was estimated at (0.29, 0.29) respectively in the CIE diagram. These nanoparticles could be used for various applications like photocatalysis, photoluminescence, electrical, and biological uses. Photoluminescence results echo the characteristic spectra of Silver nanoparticles. We hope this way of manufacturing nanoparticles could be a major source of their production.

References

[1] S. Iravani and B. Zolfaghari, BioMed Research International **2013** (2013) 639725. [*CrossRef*]
[2] J.M. Ashraf et al., Scientific Reports **6** (2016) 20414. [*CrossRef*]
[3] S.A. AL-Thabaiti et al., Colloids and Surfaces B: Biointerfaces **67**(2) (2008) 230-237. [*CrossRef*]
[4] Y.-F. Huang et al., Nanotechnology, **17**(19) (2006) 4885-4894. [*CrossRef*]
[5] W. Zhang et al., Colloids and Surfaces A: Physicochemical and Engineering Aspects **299**(1-3) (2007) 22-28. [*CrossRef*]
[6] Z. Khan et al., Colloids and Surfaces B: Biointerfaces **76**(1) (2010) 164-169. [*CrossRef*]
[7] X.-F. Zhang et al., International Journal of Molecular Sciences **17**(9) (2016) 1534. [*CrossRef*]
[8] S. Gurunathan et al., International Journal of Nanomedicine **10**(1) (2015) 4203-4223. [*CrossRef*]
[9] W.-R. Li et al., Applied Microbiology and Biotechnology **85** (2010) 1115-1122. [*CrossRef*]
[10] P. Mukherjee et al., Nano Letters **1**(10) (2001) 515-519. [*CrossRef*]

[11] A.J. Nozik, Physica E: Low-dimensional Systems and Nanostructures **14**(1-2) (2002) 115-120. [*CrossRef*]
[12] P. Yu et al., Solar Energy Materials and Solar Cells **161** (2017) 377-381. [*CrossRef*]
[13] H. Wang et al., ACS Applied Materials & Interfaces **10**(37) (2018) 30919-30924. [*CrossRef*]
[14] M. Zheng et al., Materials Research Bulletin **36**(5-6) (2001) 853-859. [*CrossRef*]
[15] J. Gao et al., Langmuir **20**(22) (2004) 9775-9779. [*CrossRef*]
[16] B.S. Siddiqui et al., Phytochemistry **53**(3) (2000) 371-376. [*CrossRef*]
[17] J. Huang et al., Nanotechnology **18**(10) (2007) 105104. [*CrossRef*]
[18] D. Shaw, Ligustrum sinense (Chinese privet), CABI Compendium (2008). [*CrossRef*]
[19] H. Jan et al., Journal of Materials Research and Technology **15** (2021) 950-968. [*CrossRef*]
[20] J. Springer et al., Journal of Applied Physics **95**(3) (2004) 1427-1429. [*CrossRef*]
[21] P. Makula et al., The Journal of Physical Chemistry Letters **9**(23) (2018) 6814-6817. [*CrossRef*]
[22] R. Singaravelan et al., Applied Nanoscience **5**(8) (2015) 983-991. [*CrossRef*]
[23] S. Khalid et al., Metal Oxide-Carbon Hybrid Materials (2022) 217-236. [*CrossRef*]
[24] A. Hendi et al., ACS Omega **5**(49) (2020) 31644-31656. [*CrossRef*]
[25] M.G. Motitswe et al., Journal of Cluster Science **32** (2021) 683-692. [*CrossRef*]
[26] K. Anandalakshmi et al., Applied Nanoscience **6** (2016) 399-408. [*CrossRef*]
[27] A. Ludwiczuk et al., Pharmacognosy: Fundamentals, Applications and Strategies (2017) 233-266. [*CrossRef*]
[28] C.S. McCamy, Science **154**(3749) 639. [*CrossRef*]
[29] Z. Huang et al., Optik **240** (2021) 166845. [*CrossRef*]
[30] A. Ghosh et al., Solar Energy **163** (2018) 537-544. [*CrossRef*]